

ARTICLES

Neuronal ensemble control of prosthetic devices by a human with tetraplegia

Leigh R. Hochberg^{1,2,4}, Mijail D. Serruya^{2,3}, Gerhard M. Friehs^{5,6}, Jon A. Mukand^{7,8}, Maryam Saleh⁹†, Abraham H. Caplan⁹, Almut Branner¹⁰, David Chen¹¹, Richard D. Penn¹² & John P. Donoghue^{2,9}

Neuromotor prostheses (NMPs) aim to replace or restore lost motor functions in paralysed humans by routing movement-related signals from the brain, around damaged parts of the nervous system, to external effectors. To translate preclinical results from intact animals to a clinically useful NMP, movement signals must persist in cortex after spinal cord injury and be engaged by movement intent when sensory inputs and limb movement are long absent. Furthermore, NMPs would require that intention-driven neuronal activity be converted into a control signal that enables useful tasks. Here we show initial results for a tetraplegic human (MN) using a pilot NMP. Neuronal ensemble activity recorded through a 96-microelectrode array implanted in primary motor cortex demonstrated that intended hand motion modulates cortical spiking patterns three years after spinal cord injury. Decoders were created, providing a 'neural cursor' with which MN opened simulated e-mail and operated devices such as a television, even while conversing. Furthermore, MN used neural control to open and close a prosthetic hand, and perform rudimentary actions with a multi-jointed robotic arm. These early results suggest that NMPs based upon intracortical neuronal ensemble spiking activity could provide a valuable new neurotechnology to restore independence for humans with paralysis.

Hundreds of thousands of people suffer from forms of motor impairment in which intact movement-related areas of the brain cannot generate movements because of damage to the spinal cord, nerves, or muscles¹. Paralyzing disorders profoundly limit independence, mobility and communication. Current assistive technologies rely on devices for which an extant function provides a signal that substitutes for missing actions. For example, cameras can monitor eye movements that can be used to point a computer cursor². Although these surrogate devices have been available for some time, they are typically limited in utility, cumbersome to maintain, and disruptive of natural actions. For instance, gaze towards objects of interest disrupts eye-based control. By contrast, an NMP is a type of brain-computer interface (BCI) that can guide movement by harnessing the existing neural substrate for that action—that is, neuronal activity patterns in motor areas. An ideal NMP would provide a safe, unobtrusive and reliable signal from the disconnected motor area that could restore lost function. Neurons in the primary motor cortex (MI) arm area of monkeys, for example, provide information about intended arm reaching trajectories^{3–5}, but this command signal would work for an NMP only if neural signals persist and could be engaged by intention in paralysed humans.

In concept, NMPs require a sensor to detect the activity of multiple neurons, a decoder to translate ensemble firing patterns into motor commands, and, typically, a computer gateway to engage effectors. BrainGate (Cyberkinetics, Inc.) is an NMP system under development

and in pilot trials in people with tetraparesis from spinal cord injury, brainstem stroke, muscular dystrophy, or amyotrophic lateral sclerosis. Currently, this system consists of a chronically implanted sensor and external signal processors developed from preclinical animal studies (see Methods)^{6–8}. The participant described in this report, the first in the BrainGate trial, is a 25-yr-old male (MN) who sustained a knife wound in 2001 that transected the spinal cord between cervical vertebrae C3–C4, resulting in complete tetraplegia (C4 ASIA A)⁹. The array was implanted in June 2004 into the MI arm area 'knob'¹⁰, as identified on pre-operative magnetic resonance imaging (MRI) (Fig. 1c). Post-operative recovery was uneventful. The data presented here are derived from 57 consecutive recording sessions from 14 July 2004 to 12 April 2005 (9 months).

Signal quality and variety

Action potentials were readily observable on multiple electrodes, indicating that MI neural spiking persists three years after SCI, as suggested indirectly by functional MRI data^{11–14}. Recorded signals ranged from qualitatively well-isolated single neurons to mixtures of a few different waveforms (Fig. 2a). Different waveform shapes were identified visually, using standard time-amplitude windows, but there was no further attempt to distinguish between well isolated and intermixed waveforms, both of which we refer to in this report as 'units'. An average of 26.9 ± 14.2 units were observed each day (range 3–57), with mean peak-to-peak spike amplitudes of $76.4 \pm 25.0 \mu\text{V}$ (mean \pm s.d., $n = 56$ sessions) (see Supplementary

¹Department of Neurology, Massachusetts General Hospital, Brigham and Women's Hospital, and Spaulding Rehabilitation Hospital, Harvard Medical School, 55 Fruit Street, Boston, Massachusetts 02114, USA. ²Department of Neuroscience and Brain Science Program, and ³Department of Engineering, Brown University, PO Box 1953, Providence, Rhode Island 02912, USA. ⁴Center for Restorative and Regenerative Medicine, Rehabilitation Research and Development Service, Department of Veterans Affairs, Veterans Health Administration, 830 Chalkstone Avenue, Providence, Rhode Island 02908, USA. ⁵Department of Clinical Neurosciences (Neurosurgery), Brown University, and ⁶Department of Neurosurgery, Rhode Island Hospital, 120 Dudley Street, Suite 103, Providence, Rhode Island 02905, USA. ⁷Department of Rehabilitation Medicine, Brown University, 593 Eddy Street, Providence, Rhode Island 02903, USA. ⁸Sargent Rehabilitation Center, 800 Quaker Lane, Warwick, Rhode Island 02818, USA. ⁹Cyberkinetics Neurotechnology Systems, Inc., 100 Foxborough Boulevard-Suite 240, Foxborough, Massachusetts 02035, USA. ¹⁰Cyberkinetics Neurotechnology Systems, Inc., 391 Chipeta Way, Suite G, Salt Lake City, Utah 84108, USA. ¹¹Department of Physical Medicine and Rehabilitation, Rehabilitation Institute of Chicago, 345 E. Superior Street, 1146, Chicago, Illinois 60611, USA. ¹²Department of Neurosurgery, University of Chicago Hospitals, 5841 S. Maryland Avenue, MC3026, Chicago, Illinois 60637, USA. †Present address: Graduate Program in Computational Neuroscience, University of Chicago, Chicago, Illinois 60637, USA.

Information)⁸. Although details of local field potentials (LFPs) will be described in a subsequent report, we note that LFPs, which could be recorded simultaneously with spikes, resembled those observed in intact monkeys (Fig. 2b)¹⁵. A notable decrease in the number of recorded units was seen approximately 6.5 months after implantation and thereafter. Upon approval of a clinical protocol change at 10 months, which permitted impedance measurements, we observed a low impedance in 54 of the electrodes, consistent with a physical short circuit to ground in the array, cable, or connector, but not consistent with a biological event (for example, gliosis). The precise reason for this physical change remains under investigation.

Since this report was written, we added a second trial participant to the study, a 55-yr-old man who has had complete spinal cord injury at C4 since 1999. Recordings were collected starting in the seventh month after implant, after making an electrical contacts repair in the pedestal connector. We recorded an average of 53.2 ± 6.3 units per session during trial months 7–10, again demonstrating the presence of neural activity lasting many months. Another technical issue causing abrupt signal loss at most electrodes, which may be related to the original repair, occurred at month 11 in participant 2; the reason for this change is being evaluated.

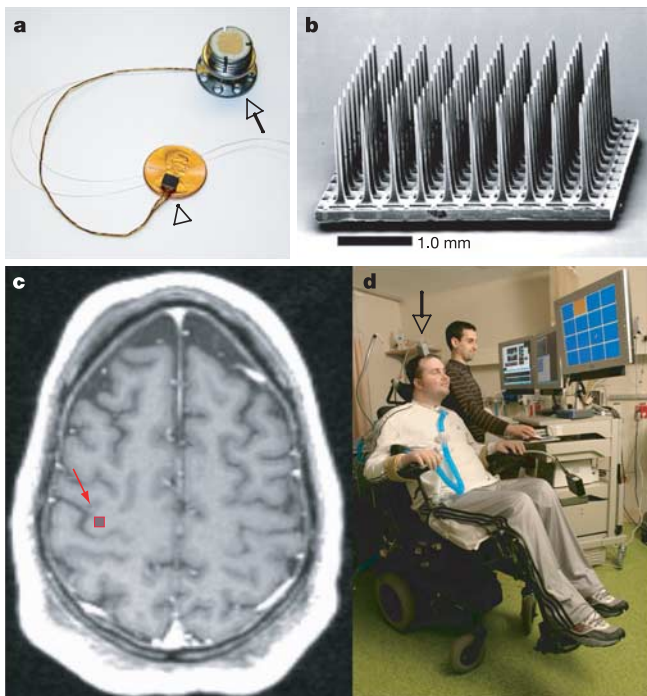


Figure 1 | Intracortical sensor and placement, participant 1. **a**, The BrainGate sensor (arrowhead), resting on a US penny, connected by a 13-cm ribbon cable to the percutaneous Ti pedestal (arrow), which is secured to the skull. Neural signals are recorded while the pedestal is connected to the remainder of the BrainGate system (seen in **d**). **b**, Scanning electron micrograph of the 100-electrode sensor, 96 of which are available for neural recording. Individual electrodes are 1-mm long and spaced $400 \mu\text{m}$ apart, in a 10×10 grid. **c**, Pre-operative axial T1-weighted MRI of the brain of participant 1. The arm/hand 'knob' of the right precentral gyrus (red arrow) corresponds to the approximate location of the sensor implant site. A scaled projection of the 4×4 -mm array onto the precentral knob is outlined in red. **d**, The first participant in the BrainGate trial (MN). He is sitting in a wheelchair, mechanically ventilated through a tracheostomy. The grey box (arrow) connected to the percutaneous pedestal contains amplifier and signal conditioning hardware; cabling brings the amplified neural signals to computers sitting beside the participant. He is looking at the monitor, directing the neural cursor towards the orange square in this 16-target 'grid' task. A technician appears (A.H.C.) behind the participant.

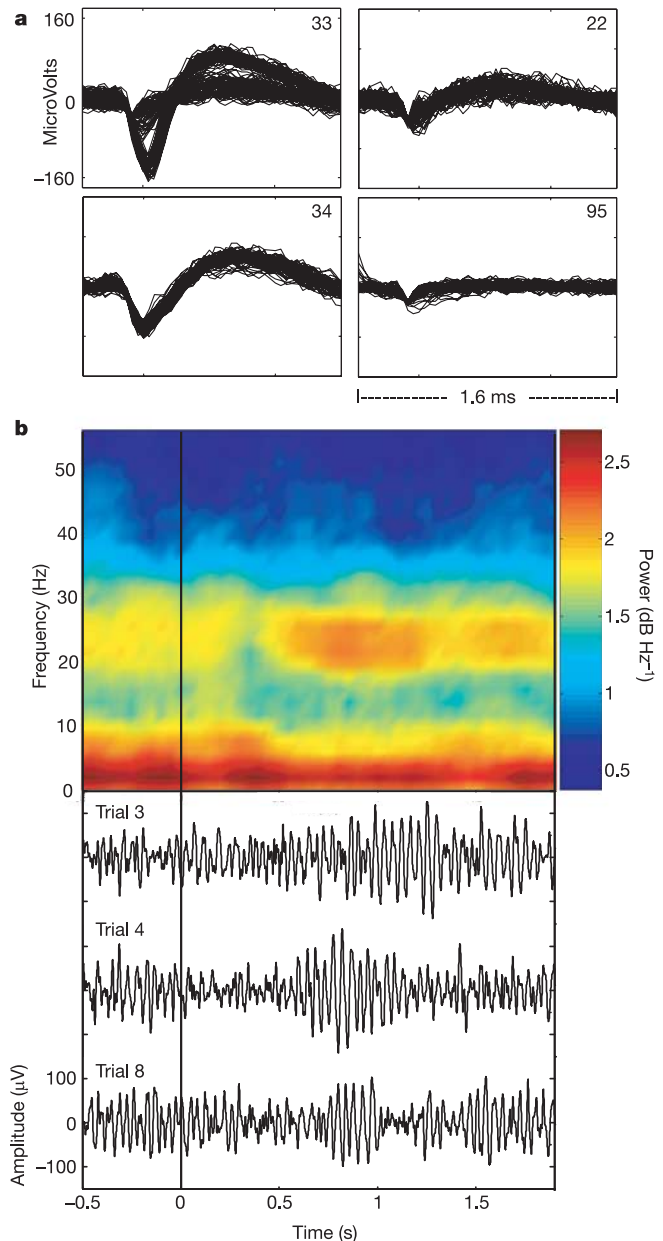


Figure 2 | Electrical recordings from a sample of four electrodes. **a**, Discriminated neural activity at electrodes 33, 34, 22, 95 ($n = 80$ superimposed action potentials for each unit). On electrode 33, two neuronal units could be reliably discriminated with peak to peak amplitudes of 206 and $56 \mu\text{V}$, respectively. For electrode 34, a single unit is displayed. Electrode 22 illustrates a low-amplitude discriminated signal. Electrode 95 shows triggered noise. Data are from trial day 90 (90 days after array placement). **b**, Local field potentials during neural cursor control. In the bottom panel, three traces of electrical recording (bandpass: 10–100 Hz) from one electrode are shown 0.5 s before and 1.9 s after the go cue instructing MN to move the cursor from the centre position to a target at the top of the screen. In the top panel, a Thomson multi-taper time frequency analysis on each trial data segment was performed. This was done by sliding a 0.3-s window every 0.05 s, using a spectral resolution of 10 Hz. These power spectrograms were averaged across 20 trials to create the resulting pseudocolour power spectral density (PSD) plot. The diagram is aligned such that each point in the PSD plot corresponds to a time window 150 ms before and after an LFP. In the 20–30-Hz band, a decrease in power is seen approximately 300 ms after the go cue, followed by an increase in power from 550–1,200 ms after the go cue, which can also be appreciated in the raw, single trial data below.

Modulation by intent

Imagined limb motions modulated neural firing on multiple electrodes, upon request, beginning at the first experimental session. Modulation was evaluated during four consecutive sessions when MN was asked to imagine a series of movements. This series revealed a rich variety of firing modulations largely consistent with patterns observed in monkey MI¹⁶. Importantly, this activity was evoked by imagined actions in this participant with cervical spinal cord injury. Figure 3a illustrates how certain neurons are selective for one imagined action (hands together/apart), whereas others recorded simultaneously are engaged by different imagined actions (elbow or wrist). This diversity includes neurons that fired with imagined hand or distal arm actions (for example, hand open/close, Fig. 3c) and those that fired during shoulder movements that were actually performed (see also Supplementary Fig. 1). Non-selective neurons, active with the onset of any imagined upper extremity action (Fig. 3b), were also observed. As shown in Fig. 3c and Supplementary

Fig. 1, neurons fired in a relatively time-locked manner upon the request to imagine action. These results demonstrate a rich heterogeneity of firing patterns within a limited sample from a small MI region. This diversity is useful in creating a flexible control signal.

Linear filter construction

Use of MI neuronal ensemble activity as a control signal by persons with paralysis requires a novel approach to establishing a transform (filter function) between firing patterns and intended action. For each session, units were used to create a filter (see Methods) to provide a two-dimensional output signal displayed as cursor position on a monitor. A simple linear filter algorithm, identical to that used in intact monkeys, was used to create filters¹⁷. Unlike most studies performed using intact monkeys, where hand motions are known and kinematics are measured directly, we predicted MN's intended hand movements on the basis of

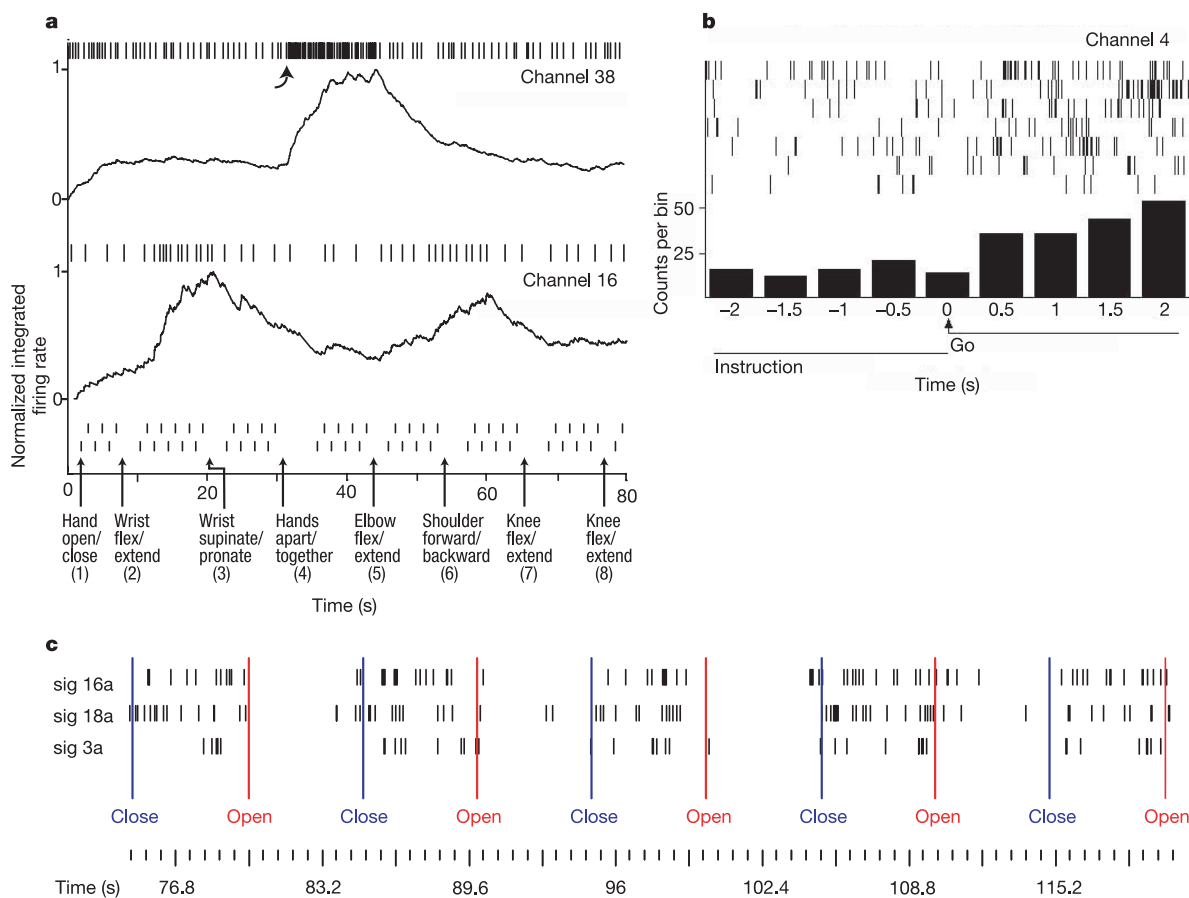


Figure 3 | Neuronal selectivity for imagined and performed movements.

a, Over an 80-s period, MN was asked to imagine performing a series of left limb movements (which are described on the abscissa). Movement instruction time is indicated by a vertical arrow; the go cue for each alternating movement, presented as text on the video monitor, is indicated by a small vertical hash mark. Spiking activity of two simultaneously recorded units is displayed. Rasters indicate the time of each spike (thinned for visual clarity; every third spike is shown). Normalized, integrated firing rates (R) appear beneath each raster, as derived by the equation $R = [(R_{-1} + n)(1 - e^{-b/\tau})]$, where R_{-1} is the previous bin's integrated firing rate value, n = the number of spikes in the current bin, b = bin width, and τ = time constant; bin width = 50-ms window, time constant = 10 ms (adapted from ref. 28); normalization is achieved by dividing by the maximum integrated firing rate from each unit's spike train over the time period displayed. The top unit (channel 38) increases its firing rate (curved arrow) with the instruction to move both hands apart/together. The bottom, simultaneously recorded unit (channel 16) is activated most clearly after the

instruction to flex/extend the wrist and to flex/extend the elbow or move the shoulder anteriorly and posteriorly. All movements are imagined except for shoulder movement, which MN actually performed. **b**, Go-cue-related activity modulation for a neuron recorded simultaneously with those in **a**. Each raster line is centred about the go cue, which requests that the patient imagine a movement; the seven raster lines represent the epochs surrounding each of the seven different movements in sequence **a**. The histogram displays the total number of spikes seen in each 500-ms bin. This neuron increased its firing rate during most imagined movement epochs, but demonstrated poor instruction selectivity compared to the neurons presented in **a**. Data are from day 161. **c**, Hand-instruction-related modulation for three simultaneously recorded neurons. MN was cued to open and close his hand by text instruction, presented on the screen. Go cues are indicated. Each vertical tick represents one action potential (spike). An increase in these neurons' firing rates is directly indicative of the intention to close the hand. Data are from day 90.

instructed actions (instruction-based algorithms have also been reported in one study of intact monkeys¹⁸). Thus, for filter building, MN was asked to imagine manually tracking a ‘technician’s cursor’ that was actually being moved by a technician-operated mouse through a succession of randomly placed visual targets (see Methods). The filter function was used to decode activity and drive a ‘neural cursor’.

MI activity during neural cursor control

Features of neurons during neural cursor control resembled those expected from MI. Neurons in MI of intact monkeys characteristically begin to modulate their firing before movement onset and activity is tuned to hand movement direction^{19–21}. To compare this neural activity with MI of a human with spinal cord injury, MN performed a step-tracking, ‘centre-out’ task using the neural cursor. The task requires that the neural cursor be moved from a centre target to one of four radially displaced targets (screen location: up, down, left, right; see Supplementary Video 1). For each of six sessions, MN performed this task by imagining hand motion (see Methods) as soon as the target cue appeared. The task was performed immediately after filter building without intervening practice. Timing and directional tuning features of MI neurons during imagined actions were consistent with those observed in MI of intact non-human primates. Figure 4 shows that spike-rate modulation occurs soon after the ‘go’ cue and that modulation varied by target location, as would be predicted for MI if actual arm motions were performed¹⁷. Furthermore, 66 out of 73 discriminated units (90.4%) significantly changed their firing rate in relation to the appearance of the go cue (Kolmogorov–Smirnov test, $\alpha = 0.05$, rate calculated over a sliding 1-s window, overlapping every 0.05 s; 60-s data set for each condition, $n = 3$ sessions). These results indicate that, even years after spinal cord injury and in the absence of kinaesthetic feedback and limb movement, MI neurons can still be actively engaged and encode

task-related information during the intention to move the limb ordinarily controlled by that MI region.

Quality of neural cursor control

Neural cursor position was significantly correlated with technician cursor position during the last block of the pursuit filter building task (x coordinate $r^2 = 0.56 \pm 0.18$ and y coordinate $r^2 = 0.45 \pm 0.15$, $n = 6$ sessions, Fig. 5). These correlations are similar or better than those seen in intact monkeys when linear filters were used to predict real-time hand position from MI neuronal ensembles^{5,22}. The neural cursor could be directed towards targets with a form qualitatively similar to that seen for intact monkeys using closed-loop neural control^{17,18,23}. As in intact monkeys, neural cursor motion had underlying instabilities and variable oscillatory components compared to hand motions of able-bodied individuals. Continuous neural cursor motion with the linear filter made cursor fixation at a single location difficult to achieve.

Data from the centre-out task were used to evaluate the speed and accuracy of cursor control, which are essential design parameters for any future practical NMP. As shown in Fig. 6, the participant correctly acquired 73–95% of targets (control 6.5%; $n = 80$, paired t -test, $P < 0.0001$, see Methods) when measured in a series of six sessions (see also Supplementary Fig. 2). Performance errors reflected both instabilities in cursor direction control and the ability to hold at the target location. Mean time to target was 2.51 ± 0.16 s (\pm s.e.m.) for successfully acquired targets. Although the best 13% of MN’s trials were within the range consistently achieved by able-bodied controls using a computer mouse ($n = 3$, mean 1.06 ± 0.08 s (\pm s.e.m.)), the distribution of times for MN using neural control is skewed to longer acquisition times (Fig. 6b). Effective use of the neural cursor in more complex spatial control tasks was evident when MN directed the cursor to randomly placed targets while attempting to avoid obstacles in the cursor’s path (see Supplementary Video 5).

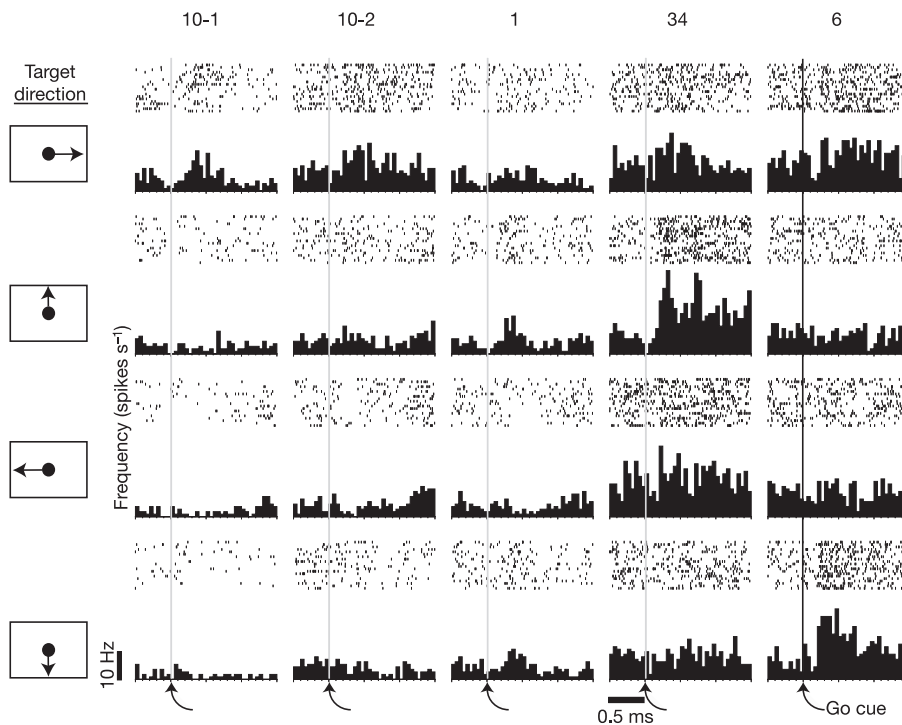


Figure 4 | Directional tuning during centre-out task. Peristimulus time histograms show spike rates for five neurons recorded simultaneously during the performance of a four-direction centre-out task (day 90) in which MN used the neural cursor to acquire a target presented at the right, top, left, or bottom of the screen. Twenty trials are displayed for each target location. Increases in activity after the go cue demonstrate movement-intention-

related modulation. Each column shows the firing of one unit in the four directions, aligned on the cue to move. Note, for example, the time-locked increase in firing of unit 6 when MN was cued to move the cursor downward (lower right corner) and the lack of change in firing rate for upward instruction. Changes in firing across the five neurons reveal directional tuning.

Further information concerning spatial and temporal accuracy was obtained from a 'grid task' (see Supplementary Information). As shown in Supplementary Video 8, participant 2 also performed the centre-out task, highlighting the ability for this second participant with spinal cord injury to modulate his motor cortical activity voluntarily for external device control. This participant's neural control, however, was generally less accurate and consistent than MN's; we are investigating the extent to which technical or other factors may underlie this performance. This and other participants' data will be reported in subsequent manuscripts.

Although he is tetraplegic, MN retains shoulder, neck and head mobility, and some recorded MI cells fired during shoulder movement

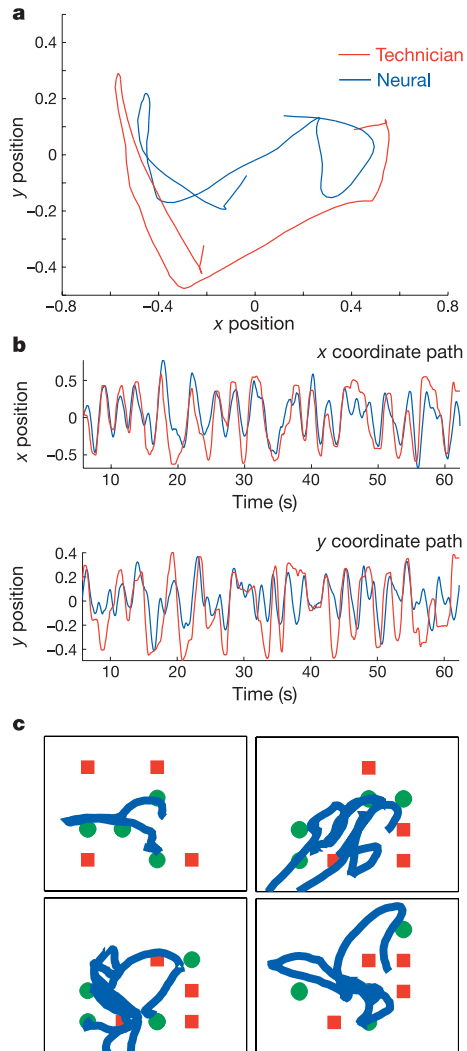


Figure 5 | Reconstruction of neural cursor position during pursuit tracking. **a**, Technician (red line) and neural cursor (blue line) paths during a 5-s epoch during which MN was asked to track the technician cursor with his neural cursor in real time. MN was able to track the general direction of the technician cursor with the neural cursor, changing directions quickly, while having some difficulty in overlaying the cursors precisely. Trial day 90. **b**, x , y position control over time during one tracking trial (last 1-min epoch of filter building). The top panel displays the x coordinate position of the technician cursor (red) and the neural cursor (blue); y positions for the same movement are shown in the bottom panel. **c**, Neural cursor position during a target acquisition/obstacle avoidance task. The four panels represent the four epochs shown in Supplementary Video 5. Green circles indicate targets; red squares indicate obstacles. The thick blue line indicates the path taken by the neural cursor and illustrates the ability to avoid most obstacles and acquire most targets within a randomly arranged field. Data are from trial day 90.

(see Supplementary Fig. 1). NMPs will nearly always operate in the context of some existing movement capabilities (given the considerable variability of remaining sensory and motor functions in people with CNS injury); thus, during filter building and use MN was not asked to remain completely still, and he sometimes moved his head or neck. It is thus possible that retained movements influenced cursor action, much as such movements are known to influence activity correlated with ordinary hand actions²⁴. These still-intact movements, however, did not appear to be essential for MN's cursor control, as can be appreciated particularly when he played 'Neural Pong' (Supplementary Video 4). In this video, movement of the head or the shoulders sometimes accompanied cursor control, but at other times MN moved the cursor purposefully while his head remained stationary, and during other epochs his head moved but the cursor motion appeared to be unrelated to head movement. We compared neural cursor position in Supplementary Video 4 to head position (both assessed by coordinates on a video playback monitor) and found no consistent relationship ($r^2 = 0.063$). This finding is inconsistent with a unique causal relation between head and cursor control. In addition, it was our repeated observation that, at least some of the time, MN performed neural control (and open-loop) tasks without moving his shoulder. Thus, based upon our instructions and MN's self-reporting that he was actively imagining arm action, we conclude that cursor motion is under the guidance of imagined/intended actions.

Direct control of prosthetic devices

Continuous computer cursor control could be used to provide many valuable new outputs for a person with paralysis to carry out

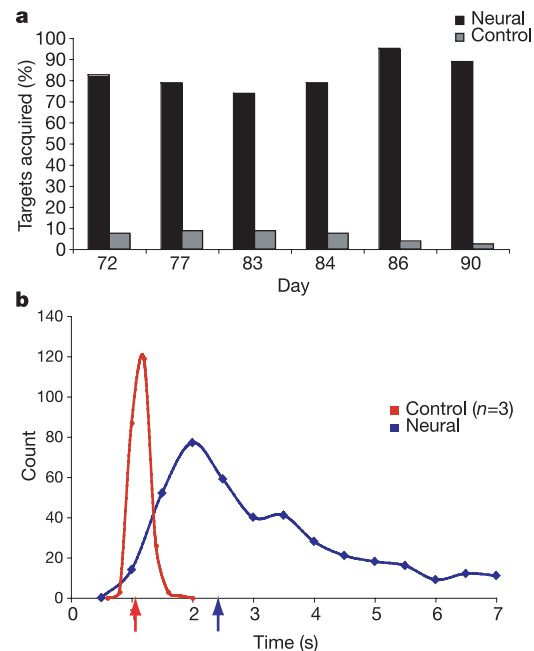


Figure 6 | Centre-out task performance. **a**, Target acquisition accuracy during the centre-out task. For each of six sessions, MN acquired between 73–95% of the radially placed targets. Control targets were not present on the monitor during task performance, but were marked as acquired if, during post-hoc analysis of the cursor movement, the cursor had traversed the location of one of the other three pseudo-randomly selected targets before the correct target (see Supplementary Video 1). Data from days 72, 77, 83, 84, 86, 90 are shown. **b**, Time-to-target performance during centre-out task for MN (blue) and three able-bodied controls (red). Only successful target acquisitions in <7 s are shown for MN. Arrows on the abscissa represent median times to target for each distribution. Controls' performances ($n = 3$ controls, 80 trials each) are collapsed into 0.2-s bins. MN's performance (398 trials) is collapsed into 0.5-s bins for visual clarity.

activities of daily living. Such a control signal could be used not only to direct computer software, but also to operate external physical assistive devices. MN tested his ability to perform potentially useful actions in a series of demonstrations.

MN used a simplified computer interface to open simulated e-mail and to draw an approximately circular figure using a paint program (Supplementary Video 2). Using the neural cursor coupled to a simple hardware interface, he adjusted the volume, channel and power to his television. He was also able to play video games such as Neural Pong (see Supplementary Videos 3–5). Control of two robotic devices was achieved, allowing MN to manipulate directly the environment. In one example, neural output was coupled to a prosthetic hand (Liberating Technologies, Inc.; see Methods) and MN was able to open and close the hand under volitional control (see Supplementary Video 6). Although only a one-dimensional form of proportional control, he achieved this action after a few trials while looking at the hand and without requiring feedback from the cursor display. Lastly, MN used a simple multi-jointed robotic limb to grasp an object and transport it from one location to another (see Supplementary Video 7 and Supplementary Information). These demonstrations illustrate transfer of control directly to a physical device without depending on continued viewing of computer cursor feedback, and suggest that manipulation of the environment to enable activities such as self-paced eating, as well as other goal-directed actions, could be achieved in tetraplegic humans.

Notably, each of these tasks was achieved rapidly and could be performed while the participant was conversing. Thus, the MI-based NMP may have the property of allowing external device control with little more disruption than encountered in able-bodied humans when they are using their arms or hands and simultaneously carrying out other motor or cognitive functions.

Discussion

The research shown here from the first participant in an ongoing pilot clinical trial provides initial evidence that a human unable to move or sense his limbs can operate a NMP using MI neuronal ensemble spiking activity as a control source. In addition, we demonstrate that neural spiking remains in the MI arm area and can be modulated by intention years after spinal cord injury. These findings provide a number of novel insights concerning cortical function and the impact of spinal cord injury in humans (see Supplementary Information).

Although MN used direct neural control to perform reasonably challenging tasks, the level of the control is considerably less than that of an able-bodied person using a manually controlled computer mouse. A number of factors might affect control, including: (1) the small set of randomly selected neurons recorded by this single array, compared to the very large number usually engaged; (2) the influence of spinal cord injury mechanisms or duration since injury; (3) the cortical layers recorded; (4) our approach to filter building; (5) the nature of the linear filter (as compared, for example, to Kalman filters²², adaptive algorithms or support vector machine approaches²⁵, not yet tested in our work); (6) attention and motivational state during filter building or control; and (7) the user interface. Changes in the recorded population across days may also contribute to both variability and instability of control. Shifting ensembles may result from small motions of the array or through other poorly understood mechanisms. Despite these variables, it is important to note that useful filters could be created daily from that neural population, and that advances in knowledge and technology are likely to improve recording and decoding. For example, cursor control might be enhanced further by adaptive algorithms or more selective choice of neural signals. Combinations of spiking activity and simultaneously recorded LFPs would provide additional signals that might improve performance.

Efforts to optimize performance may help to identify the design

criteria for a clinically useful interface for paralysed humans. For example, electroencephalogram (EEG)-based control systems have been improved by limiting trial time, re-centring the cursor location after each trial, and stopping cursor motion as soon as targets were hit²⁶. By contrast, our participant had to maintain cursor control at all times without these interface enhancements. However, we found that trial success was greater when target dwell time was decreased (grid task). Incorporation of additional feedback (for example, visual, auditory, somatosensory) may also be useful in enhancing performance²⁷.

Cursor and external device control may also be improved through learning²⁸. MI of intact animals shows learning-related plasticity^{29–32}, and such plasticity undoubtedly contributes to the acquisition of direct cortical neuronal control of an NMP. Thus, we expect that learning will further improve control, as has been reported in monkeys¹⁸. The circle drawing task (Supplementary Video 2), for example, provides some evidence of improved performance with brief practice, but a better understanding of learning will require additional, more systematic investigation.

Other human BCIs are under development³³. Foremost for comparison here is one by Kennedy and collaborators, who have reported results with their neurotrophic (cone) electrode for three humans: one with amyotrophic lateral sclerosis³⁴, one with brainstem stroke^{35,36}, and one with mitochondrial myopathy³⁶ (see Supplementary Information). In contrast to previous studies, here we present evidence that cortical ensemble patterns can be decoded and used for real-time, two-dimensional control of a computer cursor and other external devices by a person with spinal cord injury. Scalp-based EEG-driven BCIs also have been tested with some success in people with amyotrophic lateral sclerosis, spinal cord injury and other forms of paralysis^{26,27,37–39}. Such indirect systems use a substitute for motor ensembles to achieve control. Although two-dimensional control has been achieved in paraplegic patients using independent modulation of scalp-recorded signals²⁶, this system requires significant learning, concentration to the exclusion of other actions, and daily scalp sensor application, but notably, not surgical placement of the sensor. It also has limited scalability to multiple functions because two-dimensional tasks appear to engage all controllable signals. In contrast, the direct NMP can be used during natural activities such as speech, and requires minimal learning beyond filter creation. It is also plausible that NMPs could be scaled so that parallel commands could be derived simultaneously from multiple sensors each in separate cortical regions. If achieved, relatively independent outputs potentially could emanate bilaterally from arm and leg areas to allow for the reanimation of paralysed limbs via functional electrical stimulation devices.

The relative merits of EEG, transcranial⁴⁰, electrocorticographic (ECoG)^{41–43} and intracortically based BCIs (NMPs) continue to be explored and expanded^{32,33}. Myriad issues including efficacy, safety (particularly with regards to surgery), reliability, longevity, required training and support, cosmesis, cost and availability will undoubtedly affect BCI success; individuals with impairments in communication and/or mobility may prioritize these factors differently when choosing a BCI, and it is possible that combinations of techniques will provide most useful restoration of control. Current BCIs (including the NMP reported here) depend upon the insights and assistance of trained experts. The need for this assistance must be eliminated through system automation.

The goal of NMPs and other BCI research is to create safe, reliable and unobtrusive neural interfaces to devices that will restore the communication, mobility, and independence of paralysed humans. NMPs could provide significant advances over current technologies because they engage natural substrates for control (that is, the MI arm/hand area), do not encumber other actions, and do not require extensive learning. It will be important to collect results from additional participants in order to understand the generality of these statements. Improvements in the decoder and user interface

are likely to provide control closer to that achieved by able-bodied humans. The potential to use implanted sensors to 're-route' neural signals may also prove valuable in stroke and other neurological disorders where pathways are disconnected. The present NMP system incorporates a transcutaneous connection that tethers a participant to a bulky cart and requires operation by a trained technician. A wireless, implantable and miniaturized system combined with automation will be required for practical use. Emerging and available technologies appear to be sufficient to overcome these obstacles, although the challenges of creating a fully implantable system may be formidable. The current data provide initial proof of concept that spiking activity from neuronal ensembles can provide a control signal after spinal cord injury sufficient to perform at least basic operations for a human with tetraplegia, justifying further engineering efforts towards a human NMP.

METHODS

See Supplementary Information for additional Methods.

Approval for these studies was granted by the US Food and Drug Administration (Investigational Device Exemption) and the Rhode Island Hospital, New England, Rehabilitation Institute of Chicago, University of Chicago, and Spaulding Rehabilitation Hospital Institutional Review Boards. The participant described in this report has provided permission for photographs, videos and portions of his protected health information to be published for scientific and educational purposes. After completion of informed consent and medical and surgical screening procedures, the 4 × 4-mm array of electrodes was implanted into the motor cortex using a pneumatic insertion technique^{8,44}. Details of the human surgical procedure are in preparation for publication.

BrainGate system. The sensor is a 10 × 10 array of silicon microelectrodes that protrude 1 mm from a 4 × 4-mm platform (Fig. 1b). At manufacture, electrodes had an impedance of 322 ± 138 kΩ (mean ± s.d.). The array was implanted onto the surface of the MI arm/hand region; electrodes penetrate into the cortex to attempt to record neurons in intermediate layers. Recorded electrical signals pass externally through a Ti percutaneous connector, which is secured to the skull. Cabling attached to the connector during recording sessions routes signals to external amplifiers and then to a series of computers in a cart that process the signals and convert them into an output (the neural cursor) that can be viewed by the participant on a computer monitor (Fig. 1d). Currently, the system must be set up and managed by an experienced technician.

Recording sessions. Research sessions were scheduled at least once per week at the participant's residence. Sessions could be cancelled (for example, due to participant request or schedule conflict) or ended early at the participant's request. Sessions would commence with neural recording and spike discrimination, followed by filter building and structured clinical end-point (cursor control) trials. Performance of video games and external device control demonstrations followed. The electrodes and neural signals selected immediately before filter building remained constant for any given session's cursor control trials; additional neural signals (detected either with alternative spike discrimination methods, or as may have become evident during the cursor control trials) could be used during subsequent video game or external device use.

Spike discrimination. Units were manually discriminated by a technician using visual features to place time-amplitude windows on waveforms displayed within 1.6-ms windows triggered when the signal crossed a manually adjusted threshold (Fig. 2) (Cyberkinetics Central Software) while the participant was at rest. We applied no objective criteria to determine whether any particular unit (or admixture of units) recorded on one day was the same as that recorded on a subsequent day. Smaller amplitude signals were likely to have consisted of admixtures of spikes from >1 neuron. These signals were nevertheless used for sessions.

Filter building. For each session, single and multiunit data were used to create a filter to generate a two-dimensional output signal. During filter building, MN was asked to imagine moving his hand as if he were controlling a computer mouse. Specifically, he was asked to imagine tracking a cursor on the computer screen; this technician cursor was moved (by the technician) through a succession of randomly positioned targets. During the first 4 min of imagined tracking, only the technician cursor and targets were visible on the screen. An initial filter was built with the neural activity collected during this epoch, then allowing a neural cursor to be placed on the screen. MN continued to track the technician cursor with his neural cursor over a series of four 1-min blocks. The filter was updated at the end of each block. To create the final filter for the research session, neural data were used from only the four neural cursor blocks.

Linear filters were constructed from a response matrix containing the firing

rate over a 1-s history for each neuron (twenty 50-ms bins), and regressing this matrix onto technician-cursor position using a pseudoinverse technique. The least-squares formulation comprises a closed-form solution:

$$\mathbf{u} = \mathbf{R}\mathbf{f} = \mathbf{R}(\mathbf{R}^T\mathbf{R})^{-1}\mathbf{R}^T\mathbf{k}$$

where \mathbf{R} is the neural response matrix, \mathbf{f} is the linear filter, \mathbf{k} is the kinematic value (x, y position), \mathbf{T} indicates the transpose of the matrix, and \mathbf{u} is the reconstruction⁵. Software for displays was custom generated for this purpose and run on standard PC computers (Orbit Micro, dual Intel Pentium 4 Xeon processors, 2 GHz).

External devices. The robot arm was obtained from Lynxmotion, Lynx 5 Series. The electric prosthetic hand was generously provided by Liberating Technologies.

Received 22 March; accepted 6 June 2006.

- Jackson, A. B., Dijkers, M., Devivo, M. J. & Poczatek, R. B. A demographic profile of new traumatic spinal cord injuries: change and stability over 30 years. *Arch. Phys. Med. Rehabil.* **85**, 1740–1748 (2004).
- Thoumie, P. *et al.* Clinical and functional evaluation of a gaze controlled system for the severely handicapped. *Spinal Cord* **36**, 104–109 (1998).
- Humphrey, D. R., Schmidt, E. M. & Thompson, W. D. Predicting measures of motor performance from multiple cortical spike trains. *Science* **170**, 758–762 (1970).
- Schwartz, A. B., Taylor, D. M. & Tillery, S. I. Extraction algorithms for cortical control of arm prosthetics. *Curr. Opin. Neurobiol.* **11**, 701–707 (2001).
- Paninski, L., Fellows, M. R., Hatsopoulos, N. G. & Donoghue, J. P. Spatiotemporal tuning of motor cortical neurons for hand position and velocity. *J. Neurophysiol.* **91**, 515–532 (2004).
- Maynard, E. M., Nordhausen, C. T. & Normann, R. A. The Utah intracortical electrode array: a recording structure for potential brain-computer interfaces. *Electroencephalogr. Clin. Neurophysiol.* **102**, 228–239 (1997).
- Guillory, K. S. & Normann, R. A. A 100-channel system for real time detection and storage of extracellular spike waveforms. *J. Neurosci. Methods* **91**, 21–29 (1999).
- Suner, S., Fellows, M. R., Vargas-Irwin, C., Nakata, K. & Donoghue, J. P. Reliability of signals from chronically implanted, silicon-based electrode array in non-human primate primary motor cortex. *IEEE Trans. Neural Syst. Rehabil. Eng.* **13**, 524–541 (2005).
- Maynard, F. M. Jr *et al.* International standards for neurological and functional classification of spinal cord injury. American Spinal Injury Association. *Spinal Cord* **35**, 266–274 (1997).
- Yousry, T. A. *et al.* Localization of the motor hand area to a knob on the precentral gyrus. A new landmark. *Brain* **120**, 141–157 (1997).
- Lotze, M., Laubis-Herrmann, U., Topka, H., Erb, M. & Grodd, W. Reorganization in the primary motor cortex after spinal cord injury—A functional magnetic resonance (fMRI) study. *Restor. Neurol. Neurosci.* **14**, 183–187 (1999).
- Shoham, S., Halgren, E., Maynard, E. M. & Normann, R. A. Motor-cortical activity in tetraplegics. *Nature* **413**, 793 (2001).
- Sabbah, P. *et al.* Sensorimotor cortical activity in patients with complete spinal cord injury: a functional magnetic resonance imaging study. *J. Neurotrauma* **19**, 53–60 (2002).
- Mikulis, D. J. *et al.* Adaptation in the motor cortex following cervical spinal cord injury. *Neurology* **58**, 794–801 (2002).
- Donoghue, J. P., Sanes, J. N., Hatsopoulos, N. G. & Gaal, G. Neural discharge and local field potential oscillations in primate motor cortex during voluntary movements. *J. Neurophysiol.* **79**, 159–173 (1998).
- Sanes, J. N. & Donoghue, J. P. Plasticity and primary motor cortex. *Annu. Rev. Neurosci.* **23**, 393–415 (2000).
- Serruya, M. D., Hatsopoulos, N. G., Paninski, L., Fellows, M. R. & Donoghue, J. P. Instant neural control of a movement signal. *Nature* **416**, 141–142 (2002).
- Taylor, D. M., Tillery, S. I. & Schwartz, A. B. Direct cortical control of 3D neuroprosthetic devices. *Science* **296**, 1829–1832 (2002).
- Evarts, E. V. in *Handbook of Physiology* (ed. Brooks, V.) 1083–1120 (Williams and Wilkins, Baltimore, 1981).
- Georgopoulos, A. P., Kalaska, J. F., Caminiti, R. & Massey, J. T. On the relations between the direction of two-dimensional arm movements and cell discharge in primate motor cortex. *J. Neurosci.* **2**, 1527–1537 (1982).
- Humphrey, D. R. & Tanji, J. in *Motor Control: Concepts and Issues* (eds Humphrey, D. R. & Freund, H. J.) 413–443 (John Wiley, London, 1991).
- Wu, W. *et al.* Modeling and decoding motor cortical activity using a switching Kalman filter. *IEEE Trans. Biomed. Eng.* **51**, 933–942 (2004).
- Carmena, J. M. *et al.* Learning to control a brain-machine interface for reaching and grasping by primates. *PLoS Biol.* **1**, E42 (2003).
- Baker, J. T., Donoghue, J. P. & Sanes, J. N. Gaze direction modulates finger movement activation patterns in human cerebral cortex. *J. Neurosci.* **19**, 10044–10052 (1999).
- Olson, B. P., Si, J., Hu, J. & He, J. Closed-loop cortical control of direction using support vector machines. *IEEE Trans. Neural Syst. Rehabil. Eng.* **13**, 72–80 (2005).
- Wolpaw, J. R. & McFarland, D. J. Control of a two-dimensional movement signal by a noninvasive brain-computer interface in humans. *Proc. Natl. Acad. Sci. USA* **101**, 17849–17854 (2004).

27. Birbaumer, N. *et al.* A spelling device for the paralysed. *Nature* **398**, 297–298 (1999).
28. Fetz, E. E. & Baker, M. A. Operantly conditioned patterns on precentral unit activity and correlated responses in adjacent cells and contralateral muscles. *J. Neurophysiol.* **36**, 179–204 (1973).
29. Fetz, E. E. & Finocchio, D. V. Operant conditioning of specific patterns of neural and muscular activity. *Science* **174**, 431–435 (1971).
30. Jacobs, K. M. & Donoghue, J. P. Reshaping the cortical motor map by unmasking latent intracortical connections. *Science* **251**, 944–947 (1991).
31. Gandolfo, F., Li, C., Benda, B. J., Schioppa, C. P. & Bizzi, E. Cortical correlates of learning in monkeys adapting to a new dynamical environment. *Proc. Natl Acad. Sci. USA* **97**, 2259–2263 (2000).
32. Schwartz, A. B. Cortical neural prosthetics. *Annu. Rev. Neurosci.* **27**, 487–507 (2004).
33. Hochberg, L. R. & Donoghue, J. P. Sensors for brain-computer interfaces. *IEEE Eng. Med. Biol.* (in the press).
34. Kennedy, P. R. & Bakay, R. A. Restoration of neural output from a paralyzed patient by a direct brain connection. *Neuroreport* **9**, 1707–1711 (1998).
35. Kennedy, P. R., Bakay, R. A., Moore, M. M., Adams, K. & Goldwithe, J. Direct control of a computer from the human central nervous system. *IEEE Trans. Rehabil. Eng.* **8**, 198–202 (2000).
36. Kennedy, P. R., Kirby, M. T., Moore, M. M., King, B. & Mallory, A. Computer control using human intracortical local field potentials. *IEEE Trans. Neural Syst. Rehabil. Eng.* **12**, 339–344 (2004).
37. Mason, S. G., Bohringer, R., Borisoff, J. F. & Birch, G. E. Real-time control of a video game with a direct brain-computer interface. *J. Clin. Neurophysiol.* **21**, 404–408 (2004).
38. Vaughan, T. M. *et al.* Brain-computer interface technology: a review of the Second International Meeting. *IEEE Trans. Neural Syst. Rehabil. Eng.* **11**, 94–109 (2003).
39. Muller-Putz, G. R., Scherer, R., Pfurtscheller, G. & Rupp, R. EEG-based neuroprosthesis control: a step towards clinical practice. *Neurosci. Lett.* **382**, 169–174 (2005).
40. Kennedy, P. *et al.* Using human extra-cortical local field potentials to control a switch. *J. Neural Eng.* **1**, 72–77 (2004).
41. Leuthardt, E. C., Schalk, G., Wolpaw, J. W., Ojemann, J. G. & Moran, D. W. A brain-computer interface using electrocorticographic signals in humans. *J. Neural Eng.* **1**, 63–71 (2004).
42. Graitmann, B., Huggins, J. E., Levine, S. P. & Pfurtscheller, G. Toward a direct brain interface based on human subdural recordings and wavelet-packet analysis. *IEEE Trans. Biomed. Eng.* **51**, 954–962 (2004).
43. Lal, T. N., *et al.* in *Advances in Neural Information Processing Systems* (eds Saul, L. K., Weiss, Y. & Bottou, L.) (MIT Press, Cambridge, Massachusetts, 2005).
44. Rousche, P. J. & Normann, R. A. A method for pneumatically inserting an array of penetrating electrodes into cortical tissue. *Ann. Biomed. Eng.* **20**, 413–422 (1992).

Supplementary Information is linked to the online version of the paper at www.nature.com/nature.

Acknowledgements The authors thank J. Joseph and D. Morris for assistance; L. Mermel for clinical planning advice; V. Zerris and M. Park for surgical assistance; G. Polykoff for clinical trial assistance; W. Truccolo for power spectral density analysis development; and the employees of Cyberkinetics for device engineering, manufacturing and clinical trial design and management. The authors also thank MN for his participation in this trial, and the nursing staff at his assisted care facility for their assistance. The authors are grateful to M. Serra and Sargent Rehabilitation Center, the study site, for administrative support. The photograph of MN (Fig. 1) is copyright 2005 Rick Friedman. This work was supported by Cyberkinetics Neurotechnology Systems, Inc.

Author Information Reprints and permissions information is available at npg.nature.com/reprintsandpermissions. The authors declare competing financial interests: details accompany the paper on www.nature.com/nature. Correspondence and requests for materials should be addressed to J.P.D. (john_donoghue@brown.edu).